Ceramics-Silikáty 66 (3), 436-446 (2022)
www.ceramics-silikaty.cz doi: 10.13168/cs.2022.0039

DIELECTRIC MEASUREMENTS AND IMPEDANCE SPECTROSCOPY OF BA-MODIFIED $(Na_{0.5}Bi_{0.5})TiO_3$ PREPARED BY THE HYDROTHERMAL METHOD

#M. MESRAR, A. ELBASSET, N-S. ECHATOUI, F. ABDI, T. LAMCHARFI

Signals, Systems and Components Laboratory (LSSC), Faculty of Sciences and Technologies of Fez, Sidi Mohamed Ben Abdellah University, B.P. 2022, Fez, Morocco

#E-mail: mohammed.mesrar@usmba.ac.ma

Submitted June 8, 2022; accepted August 10, 2022

Keywords: $(1-x)(Na_{0.5}Bi_{0.5})TiO_{3-x}BaTiO_3$, Rietveld refinement, Hydrothermal method, Nyquist impedance plot, Diffuse ferroelectric behaviour

Sodium bismuth titanate $(Na_{0.5}Bi_{0.5})TiO_3$ perovskite is presented as a lead-free concurrent for electro-ceramic engineering technologies. In this paper, $(1-x)(Na_{0.5}Bi_{0.5})TiO_{3-x}BaTiO_3$ type ceramic materials were obtained by the hydrothermal process at a very low heat treatment temperature of around 200 °C and for times up to 24 hours. The structural, microstructural, and dielectric properties of the ceramic materials were investigated. The X-ray diffraction analysis confirms the formation of the rhombohedral phase of NBT with space group R3c. Based on the Rietveld refinement, the morphotropic phase boundary (MPB) was determined for the composition x (%) = 5 and 7. The grains increase in size from 11 to 23 µm and their distribution widens with an increasing barium concentration in the morphotropic phase boundary. The dielectric constants were measured from room temperature to 600 °C for various frequencies in the range of 1 kHz - 2 MHz. From the Nyquist impedance plot, the effect of the grain and the grain boundaries on the electrical properties was studied. At high temperatures, the Uchino law modified by Echatoui et al. allows one to describe the thermal variation of the permittivity. This diffuse character is attributed to a cationic disorder due to the distribution of Na^+/Bi^{3+} and Ba^{2+} ions in the A site.

INTRODUCTION

Currently, there is considerable interest in the development of lead-free piezoelectric systems with regard to the environment. Sodium bismuth titanate, $(Na_{0.5}Bi_{0.5}TiO_3$; (NBT), has been proposed as a potential candidate for lead-free piezoelectric ceramics based on its excellent ferroelectricity at ambient temperature. [1, 2, 3, 4] Sodium bismuth titanate is characterised by having a rhombohedral perovskite structure with (a = 5,4884 Å and c = 13,5045 Å). [5, 6] Relaxor ferroelectric materials represent a special class of disordered structures exhibiting a particular structure and properties. The structural characteristics of these relaxants are readily susceptible to modification by doping or by means of the appropriate dopants. Ferroelectric relaxor materials can be used in various devices. [7, 8, 9] They have excellent mechanical characteristics, particularly a high degree of tenacity. NBT exhibits a diffuse phase transition nature leading from its non-polar ferroelectric tetragonal transitions to its ferroelectric rhombohedral transitions. [10, 11, 12] The presence of Na^+ and Bi^{3+} ions are arranged in a disordered configuration on the 12-fold cubo-octahedral sites. Several investigations have been carried out on the evolution of the $(Na_{0.5}Bi_{0.5})TiO_3$ structure as a function of temperature. These studies have shown that there are at least two phase transitions occurring in this material. [13, 14, 15] The diversity of the interpretations of the structural studies that have already been carried out on $(Na_{0.5}Bi_{0.5})TiO_3$ clearly reveal the complexity of this material. [16] This complexity is due to the number of symmetries that can exist at room temperature, to the presence or absence of a local order, on the one hand, and, in addition, to the great variety of phase transitions generated as a function of temperature. [17] An intrinsic problem with this material is the strict control of its stoichiometry, given the high volatility of some elements present (Bi and Na). One proposed solution is to reduce the titanium content by about 3 % during the solid-state synthesis to compensate for any possible synthesis losses. In order to overcome the problems of leakage currents and stoichiometry, and to also to

improve the piezoelectric properties, $(Na_{0.5}Bi_{0.5})TiO_3$ has been modified by solid solution formations. [18] Indeed, the presence of rhombohedral symmetry below the Curie temperature suggests the possibility of obtaining a morphotropic phase boundary (MPB) by forming a solid solution with another ferroelectric material of tetragonal symmetry (in analogy with the lead zirconate titanate (PZT) system). [19, 20, 21] The morphotropic phase boundary (MPB) separating the ferroelectric phases of the rhombohedral and tetragonal structure is located at about x(%) = 5 − 7 and exhibits excellent dielectric and piezoelectric properties. The longitudinal piezoelectric coefficient d33, coupling coefficient k33, permittivity and dielectric losses reach values of the order of 125 pC/N, 0.55, 580, and 1.3 %, respectively, at room temperature. [22, 23] The purpose of the current study is to investigate the effects of the site occupancy during the doping of the NBT matrix with barium, employing a new method based on oxides (Bi_2O_3, TiO_2) and carbonates (Na_2CO_3, K_2CO_3) as a reactive source, upon the structural, microstructural, and dielectric properties of $(1-x)(Na_{0.5}Bi_{0.5})TiO_{3-x}BaTiO_3$ ceramics treated by the hydrothermal method. Particular consideration was given to the dielectric, conductivity, and impedance mechanism of (1-x)NBT-xBT over a wide temperature and frequency range. In addition, this work aims to highlight the changes in the permittivity behaviour and their relation to the phase transitions when barium is substituted for Na/Bi in $(Na_{0.5}Bi_{0.5})TiO_3$.

EXPERIMENTAL

Materials and methods

$(1-x)(Na_{0.5}Bi_{0.5})TiO_{3-x}BaTiO_3$ (abbreviated as (1-x)NBT-xBT) ceramics with (x(%) = 0, 3, 5, 6, 7, 8 and 10) were prepared by the hydrothermal method. bismuth oxide (Bi_2O_3) with a high purity (98.96 %; Sigma-Aldrich), titanium oxide (TiO_2) (98.96 %; Sigma-Aldrich), barium carbonate ($BaCO_3$) (98.96 %; Sigma-Aldrich) and sodium carbonate (Na_2CO_3) (98.96 %; Sigma-Aldrich) were the starting reagents used in the preparation. Sodium hydroxide (NaOH) (98.96 %; Sigma-Aldrich) served as a mineraliser and sodium precursor. NBT was obtained via the hydrothermal process by introducing stoichiometric amounts of the starting materials using a Teflon autoclave, V = 50 ml, and a 10 M of a NaOH solution. The chemical reaction for this synthesis is given by the Equation 1:

$$\begin{gathered} Na_2CO_3 + Bi_2O_3 + 4\,TiO_2 \rightarrow 4(Na_{0.5}Bi_{0.5})TiO_3 + CO_2\uparrow \\ + \\ BaCO_3 + TiO_2 \rightarrow BaTiO_3 + CO_2\uparrow \\ = \\ [(1-x)/4]Na_2CO_3 + [(1-x)/4]\,Bi_2O_3 + xBaCO_3 + TiO_2 \rightarrow \\ (1-x)Na_{0.5}Bi_{0.5}TiO_3\text{-}xBaTiO_3 + [(1+3x)/4]CO_2\uparrow \end{gathered} \quad (1)$$

The hydrothermal process of the (1-x)NBT-xBT based ceramics is shown in Figure 1. The reaction took place at a temperature of 200 °C and was conducted for 24 hours. Once the reaction was complete, the autoclave

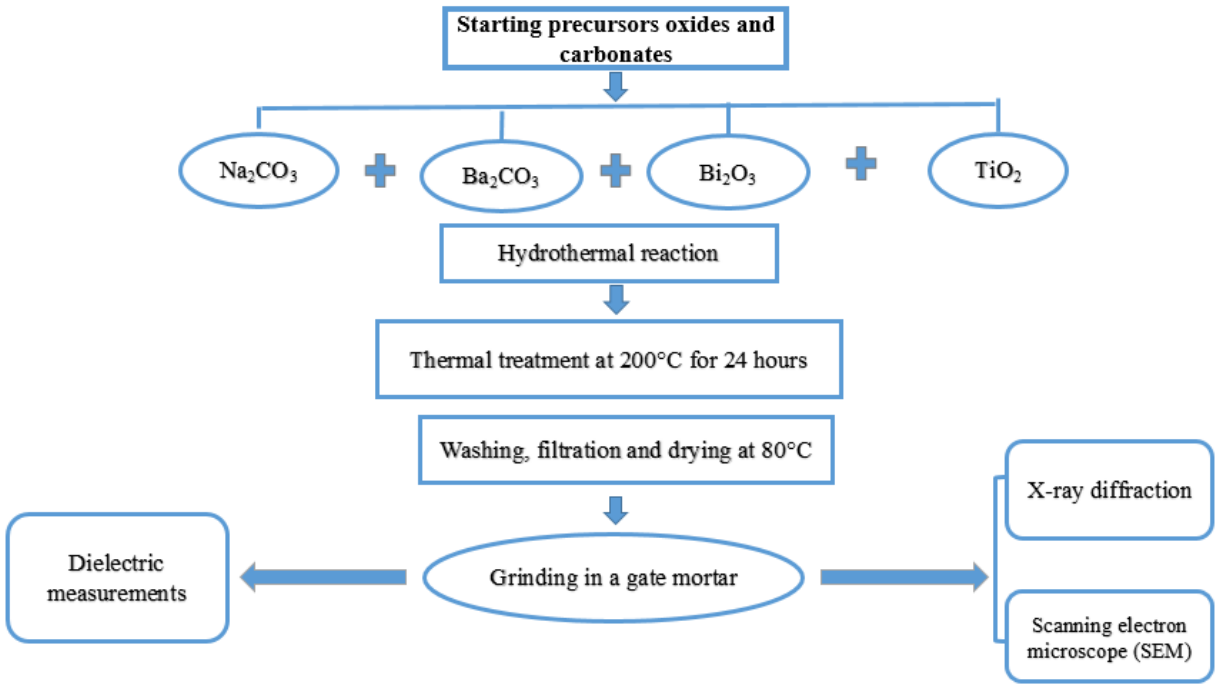

Figure 1. An illustration of the (1-x)NBT-xBT system by the hydrothermal process.

cooled naturally to room temperature. The different products were filtered, washed repeatedly with distilled water, and dried at 80 °C for 12 hours. The powders were blended with a 3 % polyvinyl alcohol (PVA) matrix and pressed into 12 mm diameter cylindrical pellets at a pressure of 8 t·cm^{-2} with a manual press. These pellets were sintered at 1000 °C for 4 hours in a resistance furnace. Crystallographic phases were obtained by X-ray diffraction, X'pert PANalytical, employing radiation, CuKα = 1.5406 Å, at ambient temperature in an angular region of 2θ = 20 - 90°.

The crystallite sizes and lattice constants were acquired using Rietveld refinements of the registered diffraction data. The microstructures of the samples were analysed by an FEI Quanta 200 EDAX scanning electron microscope (SEM). The average grain size of the ceramic samples was determined by means of Image J software. The dielectric properties, such as the loss factor, capacity, phase angle, and impedance, were measured over a broad frequency interval from 1 kHz to 2 MHz at various temperatures, 40 - 600 °C, via an Agilent 4284A impedance analyser coupled to a computer.

RESULTS AND DISCUSSION

Rietveld refinements and data analyses

Figure 2a shows the XRD patterns of the (1-x) NBT xBT ceramics with (x(%)= 0; 3, 5, 6, 7, 8, and 10) elaborated by the hydrothermal process treated at 200 °C for 24 hours with a NaOH concentration of 10 M and measured in the 2θ range of 10 – 90°. As can be seen, all the samples exhibited a pure perovskite structure and no additional second phases were identifiable within the resolution of the equipment, and show excellent agreement with the standard the Joint Committee on Powder Diffraction Standards (JCPDS) card (n°: 36–0340). [24] This also suggests that the Ba^{2+} ions dissolved into the (1-x)NBT-xBT lattice structure and then formed solid solutions. [25, 26] The Rietveld refinement method with a pseudo-Voigt analytical function was employed to refine the structural and microstructural parameters of the rhombohedral phase (space group: R3c) using the FullProf software. [27]

The Marquardt least squares approach was utilised to provide a better fit. [28] The ratio (R_{wp}/R_{exp}) referred to as the Goodness of Fit (GoF) was developed by taking the difference between the experimental (Ie) and calculated (Ic) data and minimising it. The weighted residual error and the expected residual error are the two parameters of the reliability index (R_{wp} and R_{exp}). The resulting output profiles using the Rietveld refinement are presented in Figure 2b. The refinement results obtained from the system (1-x)NBT-xBT with (x(%)= 0, 3, 5, 6, 7, 8, and 10) are:

- For x = 0 % and 3 %; the compounds have an R3c symmetry group structure, with (a = 5.487 Å, b = 5.487 Å, and c = 13.474 Å) and (a = 5.494 Å, b = 5.494 Å, and c = 13.482 Å), respectively.
- For x = 5 %, 6 %, and 7 %; the solid solution presents a mixture of two phases, rhombohedral and tetragonal, the composition of the two phases (Rh+T) varies with the Ba^{2+} content.
- For x = 8 % and 10 %; the compounds show a single-phase structure of the P4bm symmetry group.

To conclude, 0.93NBT-0.07BT exhibits a morphotropic phase boundary (MPB) at room temperature, in which rhombohedral and tetragonal symmetries coexist. Furthermore, the coexistence of tetragonal and rhombohedral phases with the P4mm and R3c space group in the morphotropic phase boundary region at room temperature has also been reported by several authors. [29, 30, 31]

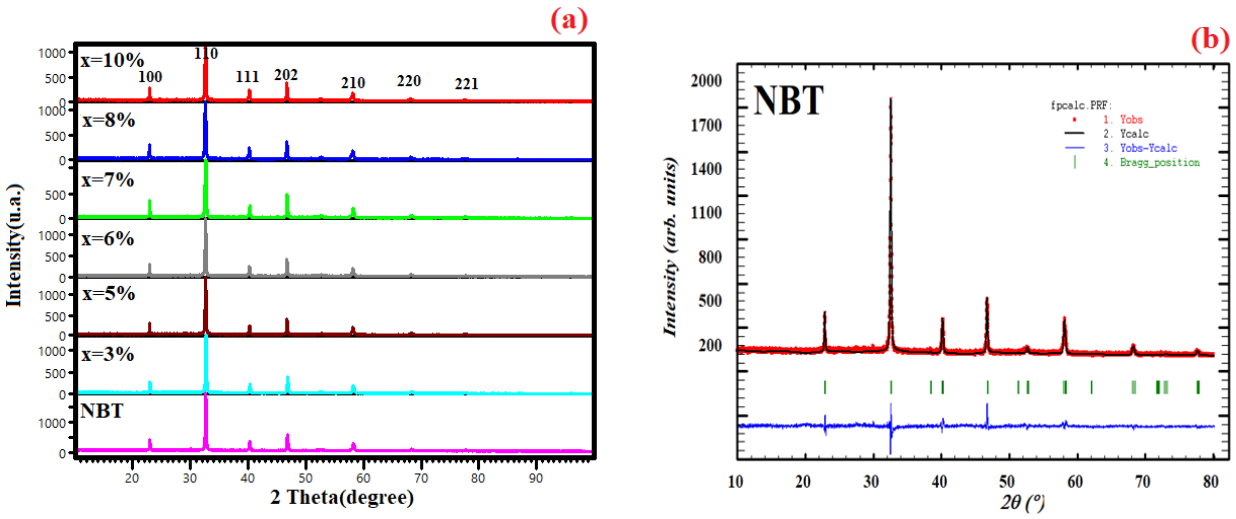

Figure 2. (a) X-ray diffraction pattern of all the sintered (1-x)NBT-xBT ceramics. (b) X-ray powder diffraction pattern by the Rietveld refinement of NBT.

The crystallite size was calculated using Scherrer's formula given below:

$$\beta_{size} = \frac{K \times \lambda}{D \times COS\theta} \quad (2)$$

Where, K = 0.9 (Scherrer constant), θ = Peak position (radians), β = Full width at half maximum (FWHM) (radians), λ = 0.15406 nm (wavelength of the X-ray sources), and D = crystallite size (nm). The obtained FWHM values and the calculated values of crystallite size are given in Table 1. The obtained values of Crystallite size (D) (nm) for (x(%)=0, 3, 5, 6, 7, 8 and 10) are 87, 88, 107, 109, 110, 105 and 103 nm, respectively. It was found that the value of D increases with the increasing percentage of barium in the solid solution which leads to the finding that due to the presence of Ba^{2+} ions, the crystallites expand compared to those of the pure NBT sample.

Micro-structural studies

Figure 3 illustrates the surface morphology of the (1-x)NBT-xBT with (x(%) = 0, 5 and 10) ceramics. This microstructure reveals grains of distinct shapes and sizes that are uniformly distributed across the surface of the materials. The grain shape and distribution are clear and indicate the polycrystalline nature of the material. The grains are irregular in size, but the grain boundaries are clearly distinct. The pure NBT has comparatively large grains, whereas the microstructures of the Ba-modified NBT are highly compact (high density) and display large grains in the barium-rich regions. It can be seen that the grain size range of the materials is between 11 and 23 µm. Nevertheless, small grains are observed in the x(%) =10 sample, this is due to both the expansion and contraction occurring in the sintering process.

Dielectric properties

Relative permittivity of the (1-x)NBT-xBT system as a function of frequency

Figure 4 shows the variation curves of the dielectric constant registered for the (1-x)NBT-xBT samples with (x(%) = 0, 3, 5, 6, 7, 8, and 10). We observe two anomalies noted A and B as a function of the frequency for all the samples. For the pure NBT ceramic, as the frequency increases, the dielectric constant steadily increases, then, in the vicinity of the anomaly noted A, it increases strongly. It passes through a maximum, corresponding to the so-called resonance frequency (fr), at this frequency, then rapidly decreases for a frequency close to the anomaly B called the anti-resonance frequency (fa). Moreover, these findings are also valid for all

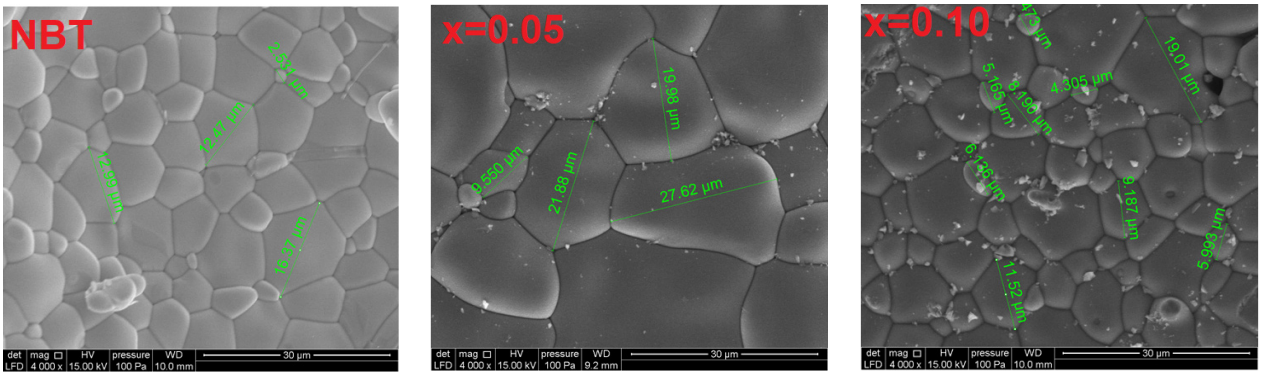

Figure 3. SEM images of the fracture surface in some re-presentative samples, of (x(%) = 0, 5 and 10) sintered at 1000 °C for 4 hours.

Table 1. Results of the refined structural parameters of the (1-x)NBT-xBT samples.

xBT(%)	Phase fraction (%)	lattice parameters			Reliability Parameters (%)			Crystallite size (D)(nm)
		a (Å)	b (Å)	c (Å)	R_{EXP} (%)	R_{WP} (%)	$\chi 2$	
0	R3c 100 %	5.487	5.487	13.474	2.65	3.90	1.47	87
3	R3c 100 %	5.494	5.494	13.482	2.63	3.17	1.20	88
5	R3c 70.125 % P4bm 29.875 %	5.501 5.498	5.501 5.498	13.488 3.910	2.26	3.25	1.43	107
6	R3c 68.267 % P4bm 31.733 %	5.514 5.514	5.514 5.514	13.492 3.930	2.15	3.18	1.47	109
7	R3c 69.763 % P4bm 30.237 %	5.519 5.515	5.519 5.515	13.514 3.941	2.32	3.78	1.62	110
8	P4bm 100 %	5.519	5.519	3.902	2.33	3.98	1.73	105
10	P4bm 100 %	5.522	5.522	3.894	2.73	3.79	1.38	103

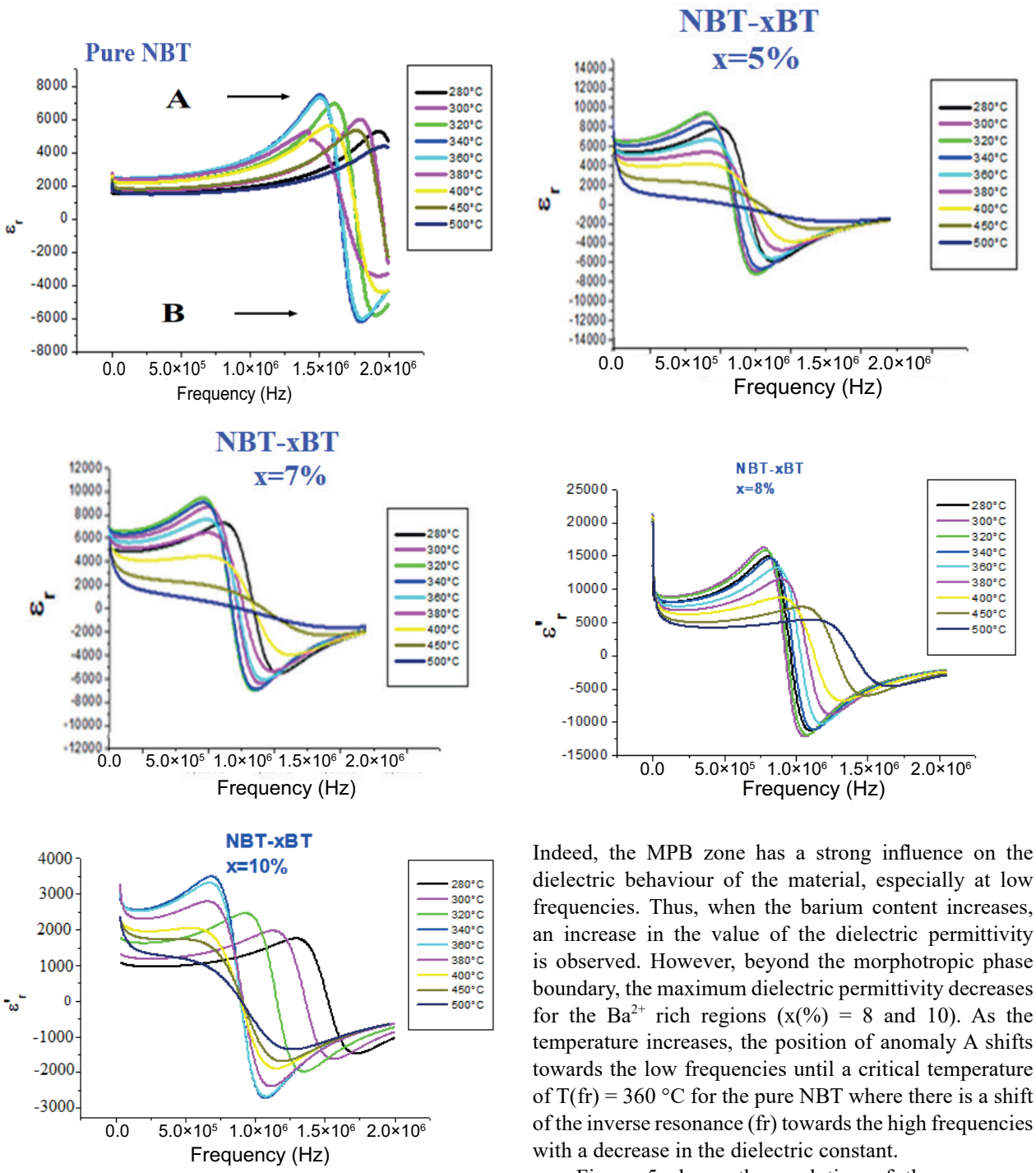

Figure 4. Frequency dependence of dielectric constant (ε') and (tan δ) at different temperatures for (1-x)NBT-xBT ceramics.

materials of the system (1-x)NBT-xBT with (x(%) = 0, 3, 5, 6, 7, 8, and 10). In contrast, ceramics belonging to the morphotropic phase boundary show colossal values of the dielectric constant at low frequencies (i.e., ≤ 10 kHz). This evolution is accompanied by a structural change resulting from the coexistence of rhombohedral (R3c) and tetragonal (P4bm) phases within this morphotropic phase boundary, confirmed by the Rietveld refinement. Indeed, the MPB zone has a strong influence on the dielectric behaviour of the material, especially at low frequencies. Thus, when the barium content increases, an increase in the value of the dielectric permittivity is observed. However, beyond the morphotropic phase boundary, the maximum dielectric permittivity decreases for the Ba^{2+} rich regions (x(%) = 8 and 10). As the temperature increases, the position of anomaly A shifts towards the low frequencies until a critical temperature of T(fr) = 360 °C for the pure NBT where there is a shift of the inverse resonance (fr) towards the high frequencies with a decrease in the dielectric constant.

Figure 5 shows the evolution of the resonance temperature T(fr) as a function of the barium content. This figure shows that the temperature T(fr) associated with the resonance decreases up to a minimum temperature T(fr) = 340 °C, then increases beyond the morphotropic phase boundary. Furthermore, the position of the resonance temperature T(fr) shifts towards low frequencies in the ferroelectric phase and towards high frequencies in the para-electric phase.

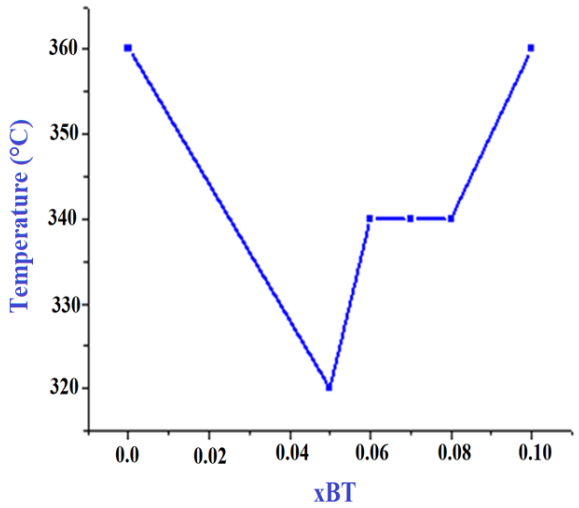

Figure 5. Evolution of the resonance temperature T(fr) as a function of the barium content.

Impedance analysis

The Nyquist plot for the complex impedance of the (1-x)NBT-xBT ceramics is presented in Figure 6. From these curves, it can be seen that the experimental points are located on half-arcs centred on the origin and having centres below the axis of the reals. The diameters of the half-arcs increase with an increasing temperature, which corresponds to the increase in the resistance value of the compounds in the morphotropic phase boundary with an increasing temperature. Thus, the material-electrode interface and the domain walls do not contribute to the electrical response. [32, 33] The presence of grain boundaries in the material generally leads to the observation of a second circular arc in the Nyquist diagram.

However, in the case of ceramics, it is possible that this second arc is not distinctly observed, it can either be masked by a deformed first circular arc, or be completely absent from the diagram, which is our case. Furthermore, the Z'' = f(Z') spectra vary with an increasing doping rate reflecting the insertion and interaction of barium with the NBT. These results seem to be in agreement with those reported by several authors. [34, 35, 36]

Diffusive phase transition

According to the literature, a frequency dependent broadening in the ɛm is associated with the diffuse phase transition. [37, 38, 39] In typically ferroelectric relaxors, notably (1-x)NBT-xBT ceramics, the diffuse phase transition phenomenon is often associated with the

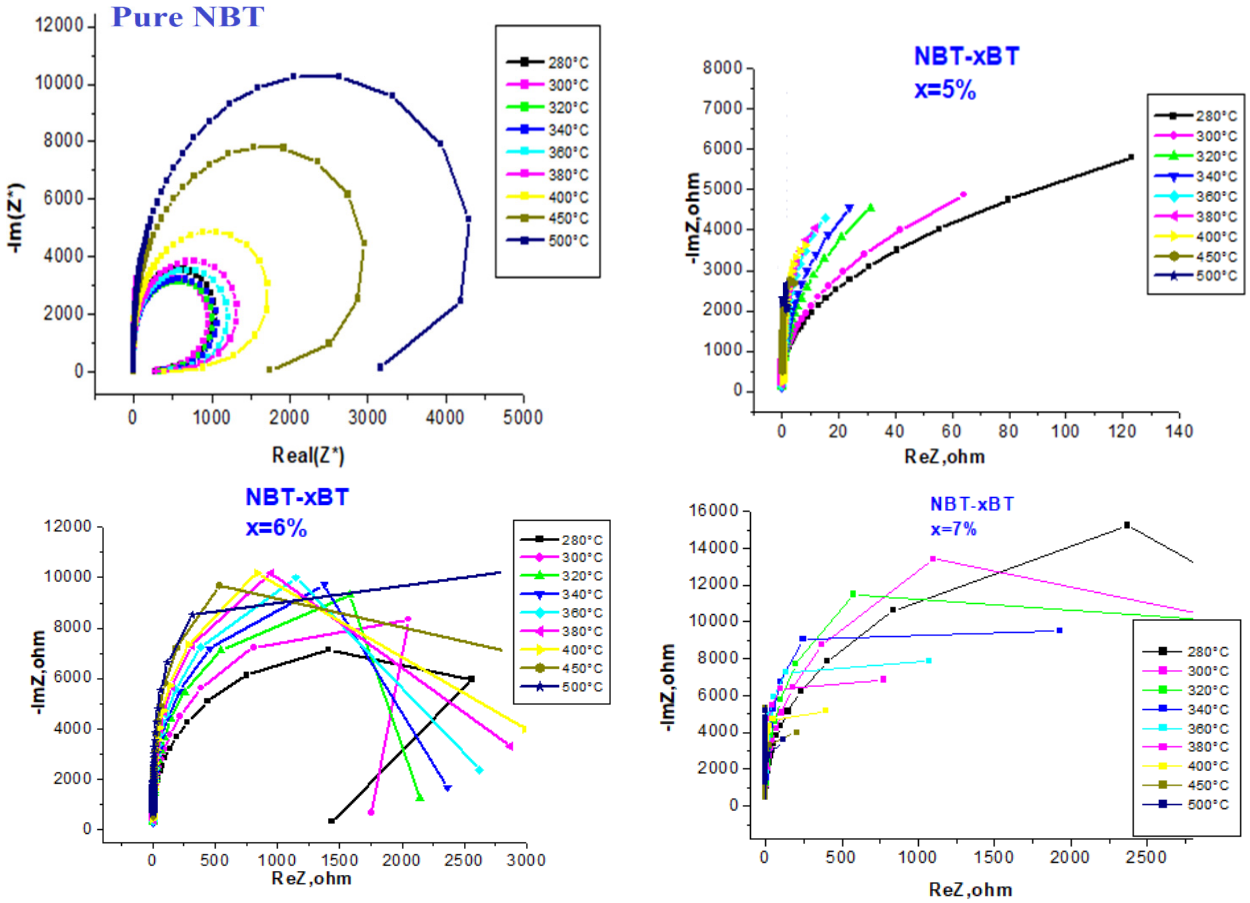

Figure 6. Plots of the imaginary part of the impedance (Im Z'') versus the real part (Z') at different temperatures (280 °C up to 500 °C) for the (1-x)NBT-xBT system.

continue on the next page ...

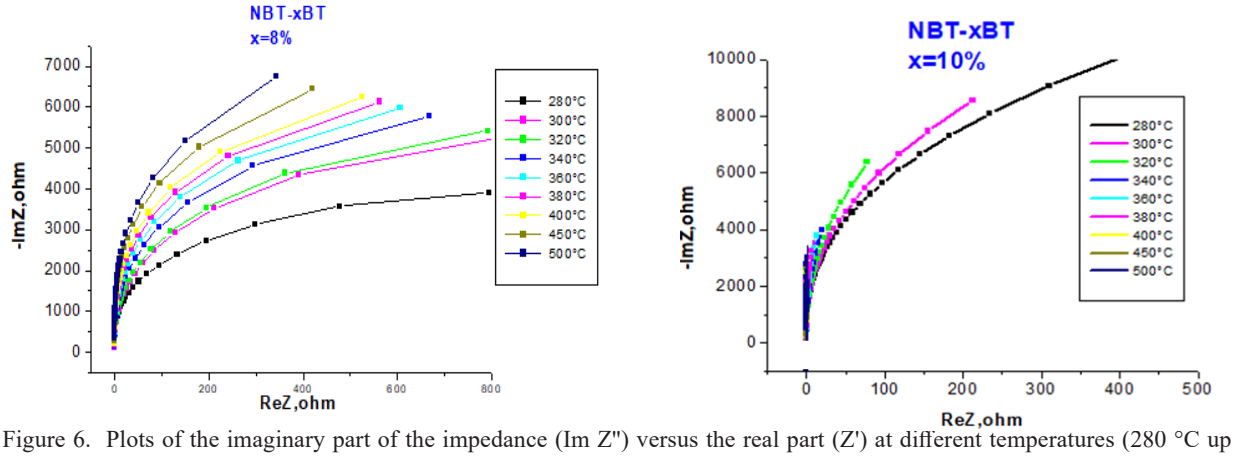

Figure 6. Plots of the imaginary part of the impedance (Im Z") versus the real part (Z') at different temperatures (280 °C up to 500 °C) for the (1-x)NBT-xBT system.

scattering of frequency measurements at temperatures below the Curie point. However, evident deviations from the Curie-Weiss law can be identified in all Ba^{2+} doped NBT materials. The degree of diffusivity γ is measured from the Uchino law modified by N.S. Echatoui et al. [40] and described as follows:

$$\frac{1}{\varepsilon_r} = \frac{1}{\varepsilon_{r\,max}}\left[1 + \frac{(T-T_m)^\gamma}{2\delta^\gamma}\right] \quad (3)$$

Where ε_{rmax} is the value of the maximum permittivity at the phase transition temperature T_m. The diffusivity parameter γ has a value of 1 for ideal ferroelectrics and 2 for relaxors. From $\mathcal{E}_{r\ max}/\mathcal{E}_r$ as a function of $(T\text{-}T_m)\gamma$, the diffusivity parameter γ is determined for a frequency of 100 kHz (Figure 7). The obtained values of γ and δ are shown in Table 2.

Table 2. Values of γ and δ as a function of the barium content of (1-x)NBT-xBT at 100 kHz.

xBT (%)	γ	δ
0	1.5	220
3	1.6	235
5	1.6	225
6	1.7	242
7	1.8	260
8	1.6	254
10	1.5	230

A typical linear correlation is obtained for this sample set; hence, it is observed that this law is verified for all the samples in this system. From the results, it can be observed that the diffusivity parameter γ increases with an increasing xBT content, from ~ 1.5 for the pure NBT to ~ 1.8 for x(%) = 7, and then starts to decrease. It is likely that the high γ values near the morphotropic transformation zone for x(%) = 7 arise from disorder within the A-site (Na^+/Bi^{3+} and Ba^{2+}). We also noticed a significant variation in the diffusion factor δ as a function of the increasing doping rate (Table 2). This clearly confirms the diffuse character of these materials.

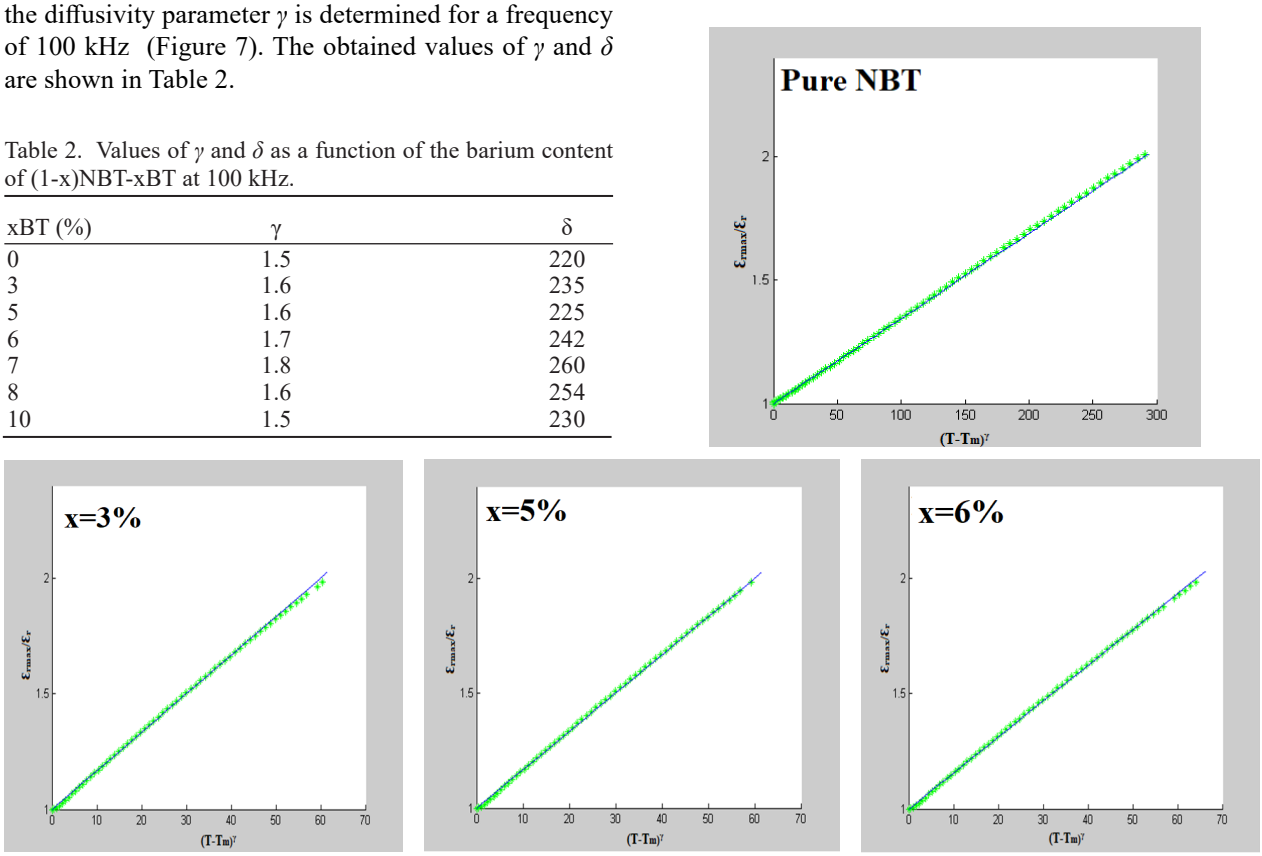

Figure 7. Modified Curie-Weiss law fit of dielectric permittivity at 100 kHz.

continue on the next page ...

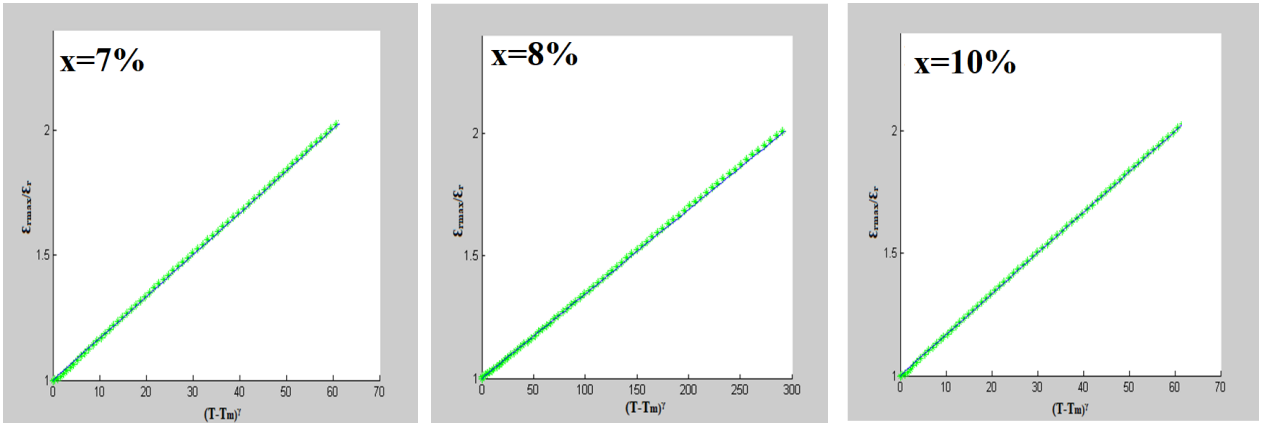

Figure 7. Modified Curie-Weiss law fit of dielectric permittivity at 100 kHz.

CONCLUSIONS

$(1-x)(Na_{0.5}Bi_{0.5})TiO_3$-$xBaTiO_3$ with (x(%) = 0, 3, 5, 6, 7, 8 and 10) ceramics were prepared by the hydrothermal method. The substitution of Ba^{2+} ions allowed a structural transition as revealed by the results of the XRD spectral analysis. The XRD results were refined by the Rietveld refinement. The implementation of a microstructural analysis verified that grain size and grain size growth were enhanced in the MPB region. The dielectric properties of ferroelectric materials sintered at 1000 °C were measured as a function of the frequency at fixed temperatures. Ceramics belonging to the morphotropic phase boundary show colossal values of the dielectric constant at low frequencies (i.e., ≤ 10 kHz). This evolution is accompanied by a structural change resulting from the coexistence of rhombohedral (R3c) and tetragonal (P4bm) phases within this (MPB) region. The existence of boundary and grain effects was examined by impedance measurements. The dielectric study reveals that the materials exhibit Ba^{2+} induced diffuse phase transition behaviour. The diffusivity increases with the Ba^{2+} content where the NBT ceramics in the (MPB) region show a higher diffusivity. We found that changing the crystal structure and microstructure of the ceramics by changing the composition leads to a significant change in the physical properties. Therefore, the change in the physical characteristics as a function of the crystal structure allows one to gain insight into the structure-property correlation.

REFERENCES

1. Ahlawat N., Rani K., Rani A. (2022): Effect of conventional and microwave sintering on microstructure and ferroelectric properties of sodium bismuth titanate (NBT) perovskite ceramics. *Materials Today: Proceedings, 54*, 895-900. doi: 10.1016/J.MATPR.2021.11.207
2. Mesrar M., Lamcharfi T., Echatoui N. S., Abdi F. (2022): $(1-x)(Na_{0.5}Bi_{0.5})TiO_3$-$x(K_{0.5}Bi_{0.5})TiO_3$ ceramics near morphotropic phase boundary: A structural and electrical study. *Materialia, 22*, 101404. doi: 10.1016/J.MTLA.2022.101404
3. Mesrar M., Lamcharfi T., Echatoui N. S., Abdi F. (2022): Effect of sintering temperature on the microstructure and electrical properties of $(Na_{0.5}Bi_{0.5})TiO_3$ processed by the sol-gel method. *Journal of Sol-Gel Science and Technology, 103*(3), 820-831. doi: 10.1007/S10971-022-05885-Y
4. Mesrar M., Elbasset A., Abdi F., Echatoui N., Lamcharfi T. (2021): Impedance spectroscopy and permittivity study of (1-x) NBT-xBT ceramics. *Ceramics–Silikáty, 66*(3), 354-364. doi: 10.13168/cs.2022.0031
5. Mesrar M., Lamcharfi T., Echatoui N., Abdi F., Harrach A. (2018): Investigation of Morphotropic Phase Boundary by Rietveld refinement and Raman Spectroscopy for $(1-x)(Na_{0.5}Bi_{0.5})TiO_3$-$xBaTiO_3$ Ceramics. *Asian Journal of Chemistry, 30*(5), 1012-1018.doi: 10.14233/ajchem.2018.21116
6. Mesrar M., Lamcharfi T., Echatoui N., Abdi F., Ahjyaje F. Z. (2019): Hydrothermal Synthesis of Oxide and Carbonate Powders of $(1-x)(Na_{0.5}Bi_{0.5})TiO_3$-$xBaTiO_3$ Ceramics. *Asian Journal of Chemistry, 31*, 309-316. doi: 10.14233/AJCHEM.2019.21581.
7. Haertling G. H. (1999): Ferroelectric ceramics: history and technology. *Journal of the American Ceramic Society, 82*(4), 797-818.doi: 10.1111/j.1151-2916.1999.tb01840.x
8. Whittle K. R., de los Reyes M., Aughterson R. D., Blackford M. G., Smith K. L., Baldo P., et al. (2018): In-situ irradiation of $Ca_{1-x}La_{2/3x}TiO_3$ defect perovskites: The role of vacancies in recovery. *Materialia, 3*, 186-191.doi: 10.1016/J.MTLA.2018.08.016
9. Minussi F. B., Reis S. P., Araújo E. B. (2021): Effects of frequency, temperature, and dc bias electric field on the dielectric properties of methylammonium lead iodide from the perspective of a relaxor-like ferroelectric. *Acta Materialia, 219*, 117235.doi: 10.1016/J.ACTAMAT.2021.117235
10. Otoničar M., Škapin S. D., Spreitzer M., Suvorov D. (2010): Compositional range and electrical properties of the morphotropic phase boundary in the $Na_{0.5}Bi_{0.5}TiO_3$–$K_{0.5}Bi_{0.5}TiO_3$ system. *Journal of the European Ceramic Society, 30*(4), 971-979. doi: 10.1016/j.jeurceramsoc.2009.10.006
11. Adhikary G. D., Khatua D. K., Senyshyn A., Ranjan R. (2019): Long-period structural modulation on the global length scale as the characteristic feature of the morphotropic phase boundaries in the $Na_{0.5}Bi_{0.5}TiO_3$ based

lead-free piezoelectrics. *Acta Materialia, 164*, 749-760. doi: 10.1016/J.ACTAMAT.2018.11.016

12. Mezilet O., Assali A., Meskine S., Boukortt A., Halati M. S. (2022): New insights into the piezoelectric, thermodynamic and thermoelectric properties of lead-free ferroelectric perovskite $Na_{0.5}Bi_{0.5}TiO_3$ from Ab initio calculations. *Materials Today Communications, 31*, 103371.doi: 10.1016/J.MTCOMM.2022.103371
13. Jones G. O., Thomas P. A. (2002): Investigation of the structure and phase transitions in the novel A-site substituted distorted perovskite compound $Na_{0.5}Bi_{0.5}TiO3$. *Acta Crystallographica Section B: Structural Science, 58*(2), 168-178.doi: 10.1107/S0108768101020845
14. Kreisel J., Glazer A. M., Bouvier P., Lucazeau G. (2001): High-pressure Raman study of a relaxor ferroelectric: The $Na_{0.5}Bi_{0.5}TiO_3$ perovskite. *Physical Review B, 63*(17), 174106. doi: 10.1103/physrevb.63.174106
15. Petzelt J., Kamba S., Fabry J., Noujni,D., Porokhonskyy V., Pashkin A., et al. (2004): Infrared, Raman and high-frequency dielectric spectroscopy and the phase transitions in $Na_{1/2}Bi_{1/2}TiO_3$. *Journal of Physics: Condensed Matter, 16*(15), 2719. doi: 10.1088/0953-8984/16/15/022
16. Petzelt J., Kamba S., Fabry J., Noujni D., Porokhonskyy V., Pashkin,A., et al. (2004): Infrared, Raman and high-frequency dielectric spectroscopy and the phase transitions in $Na_{1/2}Bi_{1/2}TiO_3$. *Journal of Physics: Condensed Matter, 16*(15), 2719. doi: 10.1088/0953-8984/16/15/022
17. Suchanicz J., Jankowska-Sumara I., Kruzina T. V. (2011): Raman and infrared spectroscopy of $Na_{0.5}Bi_{0.5}TiO_3$-$BaTiO_3$ ceramics. *Journal of electroceramics, 27*(2), 45-50. doi: 10.1007/s10832-011-9648-5
18. Hiruma Y., Nagata H., Takenaka T. (2006): Phase transition temperatures and piezoelectric properties of $(Bi_{1/2}Na_{1/2})TiO_3$–$(Bi_{1/2}K_{1/2})TiO_3$–$BaTiO_3$ lead-free piezoelectric ceramics. *Japanese journal Of Applied Physics, 45*(9S), 7409.doi: 10.1143/JJAP.45.7409
19. Shrout T. R., Zhang S. J. (2007): Lead-free piezoelectric ceramics: Alternatives for PZT?. *Journal of Electroceramics, 19*(1), 113-126.doi: 10.1007/s10832-007-9047-0.
20. Mesrar M., Lamcharfi T., Echatoui N. S., Abdi F., Harrach A. (2019): High dielectric constant of (1-x)$(Na_{0.5}Bi_{0.5})TiO_3$-x$BaTiO_3$ prepared by the hydrothermal method. *Mediterranean Journal of Chemistry, 8*(3), 213-219. doi: 10.13171/10.13171/mjc8319051210mm
21. Aman D., Abd El-Hafiz D. R., Ebiad M. A. (2018): Thermodynamic parameter for steam reforming reaction of biodiesel by-product using nano-sized perovskite catalysts. *Moroccan Journal of Chemistry, 6*(3), 6-3. doi: 10.48317/IMIST.PRSM/MORJCHEM-V6I3.6444
22. Wang X. Y., Wang C. L., Zhao M. L., Wang J. F., Yang K., Li J. C. (2007): Ferroelectric properties of lithia-doped $(Bi_{0.95}Na_{0.75}K_{0.20})_{0.5}Ba_{0.05}TiO_3$ ceramics. *Materials Letters, 61*(18), 3847-3850.doi: 10.1016/j.matlet.2006.12.045
23. Li Y., Chen W., Zhou J., Xu Q., Sun H., Xu R. (2004): Dielectric and piezoelecrtic properties of lead-free $(Na_{0.5}Bi_{0.5})TiO_3$–$NaNbO_3$ ceramics. *Materials Science and Engineering: B, 112*(1), 5-9. doi: 10.1016/j.mseb.2004.04.019
24. Dagar S., Hooda A., Khasa S., Malik M. (2020): Structural refinement, investigation of dielectric and magnetic properties of NBT doped $BaFe_{12}O_{19}$ novel composite system. *Journal of Alloys and Compounds, 826*, 154214. doi:10.1016/J.JALLCOM.2020.154214
25. Krad I., Bidault O., Geoffroy N., Maaoui M. E. (2016): Preparation and characterization of $K_{0.5}Bi_{0.5}TiO_3$ particles synthesized by a stirring hydrothermal method. *Ceramics International, 42*(3), 3751-3756. doi: 10.1016/j.ceramint.2015.10.158
26. Lim J. B., Suvorov D., Kim M. H., Jeon J. H. (2012): Hydrothermal synthesis and characterization of (Bi, K) TiO_3 ferroelectrics. *Materials Letters, 67*(1), 286-288. doi: 10.1016/J.MATLET.2011.09.094
27. Kaswan K., Agarwal A., Sanghi S., Singh O. (2015). Rietveld refinement and dielectric properties of $(Na_{0.5}Bi_{0.5}TiO_3)$-$(Bi_{0.8}Ba_{0.2}FeO_3)$ ceramics. In *AIP conference proceedings* (Vol. 1665, No. 1, p. 140014). AIP Publishing LLC.doi: 10.1063/1.4918223
28. Bellavia S., Gratton S., Riccietti E. (2018): A Levenberg–Marquardt method for large nonlinear least-squares problems with dynamic accuracy in functions and gradients. *Numerische Mathematik, 140*(3), 791-825. doi: 10.1007/s00211-018-0977-zï
29. Swain S., Kar S. K., Kumar P. (2015): Dielectric, optical, piezoelectric and ferroelectric studies of NBT–BT ceramics near MPB. *Ceramics International, 41*(9), 10710-10717. doi: 10.1016/J.CERAMINT.2015.05.005
30. Kumari R., Ahlawat N., Agarwal A., Sanghi S., Sindhu M., Ahlawat N. (2016): Phase transformation and impedance spectroscopic study of Ba substituted $Na_{0.5}Bi_{0.5}TiO_3$ ceramics. *Journal of Alloys and Compounds, 676*, 452-460. doi: 10.1016/j.jallcom.2016.03.088
31. Shi Z., Sun L., Liu K., Zhang Y., Wang W., Jiang W. (2019): Two-step hydrothermal synthesis of well-dispersed $(Na_{0.5}Bi_{0.5})TiO_3$ spherical powders. *Journal of Nanomaterials, 2019*. doi: 10.1155/2019/4768069
32. Rao K. S., Tilak B., Rajulu K. C. V., Swathi A., Workineh H. (2011): A diffuse phase transition study on Ba^{2+} substituted $(Na_{0.5}Bi_{0.5})TiO_3$ ferroelectric ceramic. *Journal of Alloys and Compounds, 509*(25), 7121-7129.doi: 10.1016/j.jallcom.2011.04.021
33. Siny I. G., Husson E., Beny J. M., Lushnikov S. G., Rogacheva E. A., Syrnikov P. P. (2000): Raman scattering in the relaxor-type ferroelectric $Na_{1/2}Bi_{1/2}TiO_3$. *Ferroelectrics, 248*(1), 57-78.doi: 10.1080/00150190008223669
34. Elbasset A., Lamcharfi T. D., Abdi F., Sayouri S. (2014): Effect of heat treatment time on the dielectric properties of BST. *Advances in Physics Theories and Applications, 30*, 2225-0638.
35. Zhao Y., Hao X., Li M. (2014): Dielectric properties and energy-storage performance of $(Na_{0.5}Bi_{0.5})TiO_3$ thick films. *Journal of alloys and compounds, 601*, 112-115. doi:10.1016/j.jallcom.2014.02.137
36. Elbasset,A., Abdi F., Lamcharfi T., Sayouri S., Abarkan M., Echatoui N. S., Aillerie M. (2015): Influence of Zr on Structure and Dielectric Behavior of $BaTiO_3$ Ceramics. *Indian Journal of Science and Technology, 8*(13), 1-6. doi: 10.17485/ijst/2015/v8i13/56574
37. Mesrar M., Lamcharfi T., Echatoui N. S., Abdi F., Ahjyaje F. Z., Haddad M. (2019): Effect of barium doping on electrical and electromechanical properties of (1-x)$(Na_{0.5}Bi_{0.5})$ TiO_3-x$BaTiO_3$. *Mediterranean Journal of Chemistry, 8*(3), 198-208.doi: 10.13171/10.13171/mjc8319050908mm
38. Mohanty H. S., Kumar A., Sahoo B., Kurliya P. K., Pradhan D. K. (2018): Impedance spectroscopic study on microwave sintered $(1-x)Na_{0.5}Bi_{0.5}TiO_3$–x$BaTiO_3$ ceramics. *Journal of Materials Science: Materials in Electronics, 29*(8), 6966-

6977. doi: 10.1007/s10854-018-8683-2

39. Omari L. H., Sayouri S., Lamcharfi T., Hajji L. (2015): Study of dielectric relaxation and diffuseness character of sol-gel derived $Pb_{1-x}La_x(Fe_{0.03}Ti_{0.97})O_3$ ceramics synthesized at lower temperature for modern nano-technological devices. *Journal of Electroceramics, 34*(1), 28-37.doi: 10.1007/S10832-014-9921-5/FIGURES/12
40. Echatoui N. S., Lamcharfi T., Sayouri S., Hajji L., Alimoussa A. (2005): Diffuse phase transition and relaxation behavior in hydrothermally processed PLZT ceramics. *Physical & chemical news*, (26), 40-46.